Journal of Mathematical Chemistry 23 (1998) 197–227

Some aspects of the symmetry and topology of possible carbon allotrope structures

R.B. King

Department of Chemistry, University of Georgia, Athens, GA 30602, USA
E-mail: rbking@sunchem.chem.uga.edu

Elemental carbon has recently been shown to form molecular polyhedral allotropes known as fullerenes in addition to the familiar graphite and diamond known since antiquity. Such fullerenes contain polyhedral carbon cages in which all vertices have degree 3 and all faces are either pentagons or hexagons. All known fullerenes are found to satisfy the isolated pentagon rule (IPR) in which all pentagonal faces are completely surrounded by hexagons so that no two pentagonal faces share an edge. The smallest fullerene structures satisfying the IPR are the known truncated icosahedral C_{60} of I_h symmetry and ellipsoidal C_{70} of D_{5h} symmetry. The multiple IPR isomers of families of larger fullerenes such as C_{76}, C_{78}, C_{82} and C_{84} can be classified into families related by the so-called pyracylene transformation based on the motion of two carbon atoms in a pyracylene unit containing two linked pentagons separated by two hexagons. Larger fullerenes with 3ν vertices can be generated from smaller fullerenes with ν vertices through a so-called leapfrog transformation consisting of omnicapping followed by dualization. The energy levels of the bonding molecular orbitals of fullerenes having icosahedral symmetry and $60n^2$ carbon atoms can be approximated by spherical harmonics. If fullerenes are regarded as constructed from carbon networks of positive curvature, the corresponding carbon allotropes constructed from carbon networks of negative curvature are the polymeric schwarzites. The negative curvature in schwarzites is introduced through heptagons or octagons of carbon atoms and the schwarzites are constructed by placing such carbon networks on minimal surfaces with negative Gaussian curvature, particularly the so-called P and D surfaces with local cubic symmetry. The smallest unit cell of a viable schwarzite structure having only hexagons and heptagons contains 168 carbon atoms and is constructed by applying a leapfrog transformation to a genus 3 figure containing 24 heptagons and 56 vertices described by the German mathematician Klein in the 19th century analogous to the construction of the C_{60} fullerene truncated icosahedron by applying a leapfrog transformation to the regular dodecahedron. Although this C_{168} schwarzite unit cell has local O_h point group symmetry based on the cubic lattice of the D or P surface, its larger permutational symmetry group is the PSL(2,7) group of order 168 analogous to the icosahedral pure rotation group, I, of order 60 of the C_{60} fullerene considered as the isomorphous PSL(2,5) group. The schwarzites, which are still unknown experimentally, are predicted to be unusually low density forms of elemental carbon because of the pores generated by the infinite periodicity in three dimensions of the underlying minimal surfaces.

1. Introduction

Two allotropes of elemental carbon have been recognized since antiquity, namely, diamond and graphite. The structure of diamond [7] (figure 1(a)) consists of an infinite three-dimensional lattice of sp^3 (tetrahedral) carbon atoms, each of which is bonded to four other carbon atoms to form interlocking six-membered C_6 rings similar to those in cyclohexane or adamantane with C–C distances of 1.514 Å. The structure of graphite [55,59] (figure 1(b)) consists of planar layers of hexagons of sp^2 (trigonal) carbon atoms with a separation of 3.35 Å between layers. The strong chemical bonding of the diamond structure in all three directions is responsible for the extreme hardness of diamond whereas the relatively slight forces between the hexagonal layers in the graphite structure are consistent with its softness and lubricity.

Until the 1980's diamond and graphite were the only allotropes of carbon which had been isolated and characterized. However, during the 1980's new allotropes of carbon were discovered exhibiting finite molecular cage structures rather than the infinite polymeric structures found in diamond and graphite. The first such molecular carbon allotrope was C_{60}, which was postulated and then shown to have a truncated icosahedral structure resembling a soccer ball with 60 vertices, 90 edges, 12 pen-

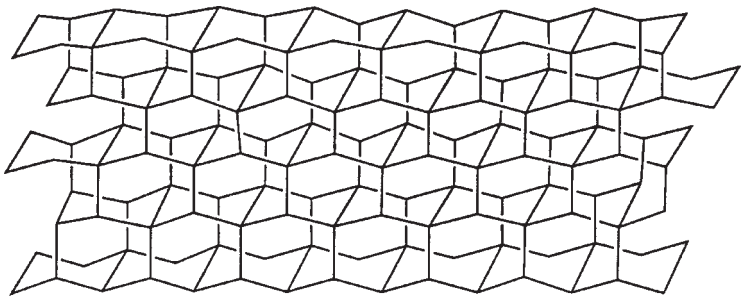

(a) Diamond

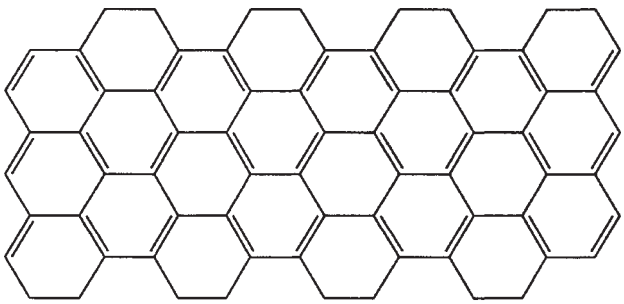

(b) Graphite

Figure 1. (a) A portion of the diamond lattice; (b) A portion of a planar hexagonal sheet of the graphite structure.

tagonal faces, 20 hexagonal faces and icosahedral symmetry (I_h) [48]. The carbon allotrope C_{60} thus provided the first example of a "hollow-shell graphite molecule" of a type first suggested by Jones in 1966 [32]. The possibility of an actual truncated icosahedral C_{60} molecule was first suggested in 1970 by Osawa in publications which were largely ignored, at least partially, because they were written in Japanese [58,70]. Subsequent publications in 1973 [5] by Bochvar and Gal'pern and in 1981 by Davidson [11] provided Hückel-type calculations of the molecular orbital energy levels of truncated icosahedral C_{60} by various methods even though there was no experimental evidence at that time for the existence of C_{60}. Initial experimental evidence for C_{60} based on the prevalence of an unusually strong m/e 720 peak in the mass spectra of soots obtained by the laser vaporization of graphite was reported by Kroto et al. [49] in 1985. Macroscopic quantities of C_{60} were first isolated by Krätschmer et al. [46] in 1990 from the soot obtained by arc-processed graphite. The truncated icosahedral structure of C_{60} was observed directly by Hawkins et al. [26] in 1991 in a single-crystal X-ray diffraction study of its adduct $C_{60}(OsO_4)(t\text{-}BuC_5H_4N)$. The introduction of the OsO_4 substituent facilitated the structural determination of C_{60} by X-ray diffraction

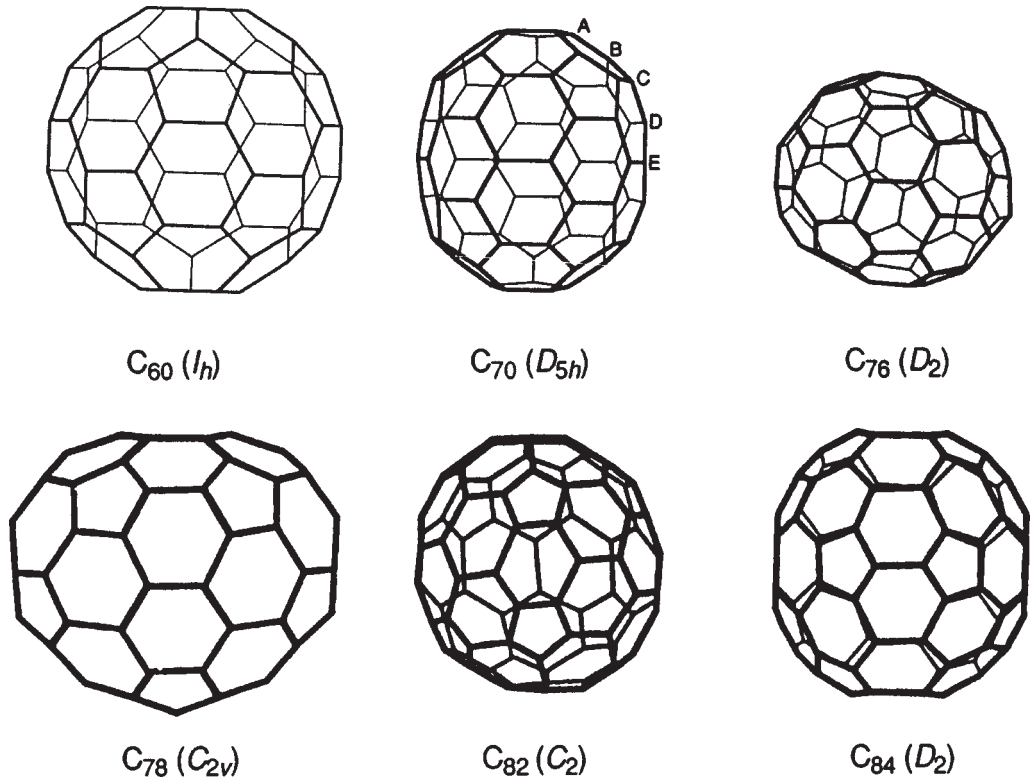

Figure 2. The fullerene polyhedra for isomers of C_n (n = 60, 70, 76, 78, 82 and 84) that have been isolated and characterized by X-ray diffraction and/or ^{13}C NMR. Examples of the five different types of carbon atoms in C_{70} are labelled A–E.

since it eliminated crystallographic disorder by reduction of the icosahedral symmetry to a lower symmetry.

The discovery of C_{60} was followed almost immediately by the discovery of other molecular C_n allotropes (e.g., $n = 70$, 76, 78, 80, 82, 84, 86, 88, 90 and 96) exhibiting other polyhedral cage structures albeit with much lower symmetry [13]. Figure 2 depicts the structures of some of these molecular carbon cages, which are generally called *fullerenes* in view of their resemblance to the architectural creations of R. Buckminster Fuller. More precisely, *a fullerene is defined as a polyhedral carbon cage in which all vertices have degree 3 and all faces are either pentagons or hexagons.* In this context, the degree of a vertex is defined as the number of edges meeting at that vertex. The fullerene cages are all found to have exactly 12 pentagonal faces, no pair of which share any edges. Various aspects of the development of fullerene chemistry are summarized in a number of review articles [47,48] and books [4,9]. The renaissance of elemental carbon chemistry arising from the discovery of fullerenes is raising new and interesting mathematical questions relating to their topologies and symmetries. Such mathematical questions are providing new opportunities for mathematical chemists, some of which are summarized in this article.

2. Fullerenes: molecular carbon cages

2.1. The topology of fullerene polyhedra

Schmalz, Klein and their collaborators [51,60] have considered possible criteria for polyhedra forming stable carbon cages having no external groups and hence corresponding to allotropes of elemental carbon. The cages are considered to be constructed by bending planar carbon networks upon themselves in two directions. The resulting carbon polyhedra thus have the following features:

(1) A three-valent σ-bonded surface corresponding to sp^2 carbon atoms with an extra p orbital to participate in delocalization leading to resonance stabilization.

(2) A carbon cage topologically homeomorphic to a sphere, i.e., no "doughnut holes" as in a torus.

(3) All carbon rings (i.e., polyhedral faces) are pentagons and hexagons to minimize ring strain and non-aromatic rings.

Some structural motifs in such fullerene polyhedra are depicted in figure 3. These structural motifs are given names corresponding to the trivial name of the simplest polycyclic hydrocarbon containing the structural motif in question.

Let us now consider some topological aspects of possible fullerene structures. The restriction to three σ bonds from each carbon vertex in the polyhedral surface relates the number ν of vertices to the number e of edges by the following equation:

$$2e = 3\nu. \tag{1}$$

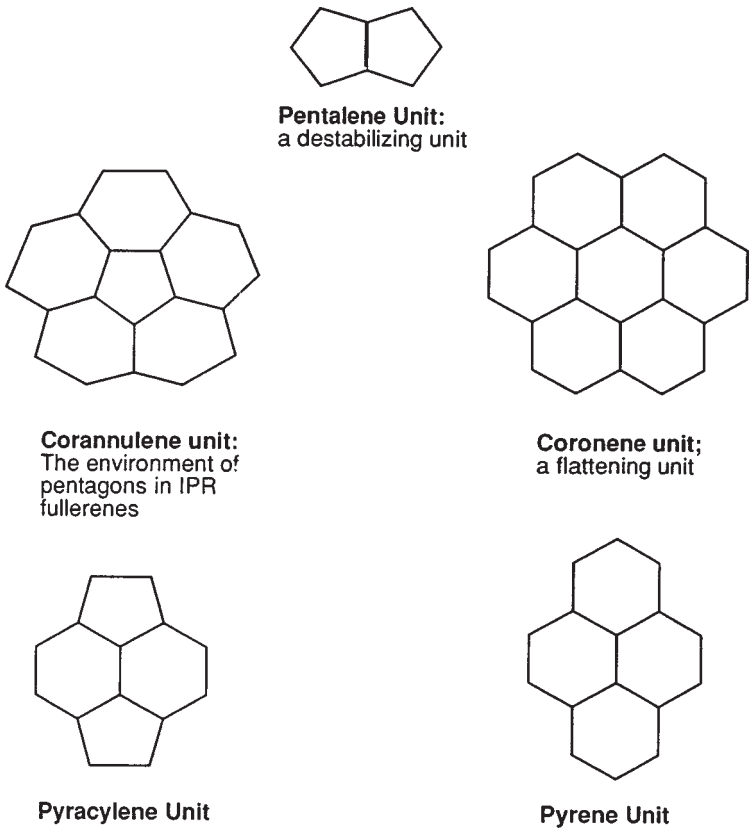

Figure 3. Building blocks for fullerene polyhedra.

Furthermore, the numbers of vertices (ν), edges (e), and faces (f) in a polyhedron homeomorphic to a sphere must satisfy Euler's relationship

$$\nu - e + f = 2. \tag{2}$$

Combining equations (1) and (2) gives the following two equations in which f_n is the number of n-sided faces (or rings):

$$\sum_n n f_n = 2e, \tag{3}$$

$$\nu + \sum_n f_n = e + 2. \tag{4}$$

Eliminating e and ν from equations (1)–(4) gives a required balance between smaller and larger rings in a carbon cage described by the following equation:

$$3f_3 + 2f_4 + f_5 - \sum_n (n-6) f_n = 12. \tag{5}$$

Equation (5) expresses the fact that 12 "units of curvature" are needed to close a graphite sheet into a cage homeomorphic to a sphere. Furthermore, equation (5) shows that these units of curvature can be made up with minimum deviation from the hexagonal rings of graphite by using exactly 12 pentagons in accord with criterion 3 above. In this connection set $f_n = 0$ except for $n = 5$, 6 and 7 to give

$$f_5 - f_7 = 12 \tag{6}$$

and

$$f_6 + 2f_7 = \frac{1}{2}\nu - 10. \tag{7}$$

Setting f_6 and f_7 to zero in equations (6) and (7) leads to the regular dodecahedron which has the 12 pentagonal faces implied by equation (6) and the 20 vertices implied by equation (7). Note that since f_6 does not appear in equation (6), fullerene polyhedra with only pentagonal and hexagonal faces, all vertices of degree 3, and 12 pentagonal faces will satisfy equation (6) with any number of hexagonal faces. Motzkin and Grünbaum [24] have proven the following theorem relating to possible fullerenes satisfying these topological criteria:

Motzkin–Grünbaum theorem. For every even vertex count with $\nu \geqslant 24$ there exists at least one fullerene containing only pentagonal and hexagonal faces (and all vertices of degree 3) and the smallest fullerene has a regular dodecahedral structure with $\nu = 20$.

2.2. The isolated pentagon rule

These elementary topological concepts used alone predict a large number of possible fullerenes including fullerenes as small as C_{20}. Additional concepts must be introduced to select a limited number of preferred fullerene structures from this large number of possible fullerene structures and to rationalize the observation of C_{60} rather than C_{20} as the smallest isolable fullerene. In this connection an important additional concept for determining fullerene structures is the so-called *isolated pentagon rule* (IPR) [60] which avoids the destabilizing 8-membered pentalene-type cycle around any two pentagonal faces sharing an edge as depicted in figure 3. Such pentalene units are destabilizing for the following reasons:

(1) The Hückel criteria for aromaticity favors cycles containing $4k + 2$ rather than $4k$ π-electrons, where k is an integer. Pentalene units have 8 π-electrons which is an unstable "4k-type" number.

(2) Topological and geometrical considerations suggest that hexagonal faces favor flat surfaces (e.g., graphite) whereas pentagonal faces form curved surfaces (e.g., the regular dodecahedron). Thus pentagonal faces lead to positive curvature whereas hexagonal faces favor zero curvature. Fusing two pentagonal faces by sharing an

edge concentrates much of the curvature of the polyhedral surface into a limited region leading to unnecessary strain in the corresponding fullerene.

Klein [42,43] has proven the following theorem concerning the IPR:

IPR fullerene theorem. For every even vertex count $\nu \geqslant 70$ there exists at least one fullerene satisfying the IPR and the smallest fullerene satisfying the IPR is the truncated icosahedron with $\nu = 60$.

Experimental observations are in excellent agreement with this theorem since the smallest isolable fullerene has been found to be C_{60} and the next higher isolable fullerene is C_{70}.

The IPR eliminates most otherwise possible fullerene structures leaving only single structures for C_{60}, C_{70} and C_{72}, two structures for C_{76}, and excludes all other possible structures for C_n fullerenes where $n \leqslant 70$ (table 1). However, for larger fullerenes C_n ($n > 76$) the number of possible structures obeying the IPR can still be large. For example, 24 possible fullerene structures for C_{84} satisfy the IPR indicating the need for additional concepts to classify such fullerene structures. In this connection fullerenes can be organized into families related by the so-called pyracylene or Stone–Wales transformation based on motion of two carbon atoms in a pyracylene unit (figure 4) [14,19,67]. Fullerenes satisfying the IPR are assumed to undergo facile in-

Table 1
Properties of fullerene polyhedra.[a]

Fullerene	Number of pentagonal faces	Number of hexagonal faces	Number of IPR structures[b]	Symmetries of IPR isomers	Number of different vertices[c]
C_{60}	12	20	1	I_h	1
C_{70}	12	25	1	D_{5h}	5
C_{72}	**12**	**26**	**1**	***D_{6h}***	**4**
C_{74}	**12**	**27**	**1**	***D_{3h}***	**9**
C_{76}	12	28	2	T_d^{d}, D_2	19 (D_2)
C_{78}	12	29	5 (1 + 4)	D_{3h} (2), D_3, $C_{2\nu}$ (2)	13 (D_3), 21 or 22 ($C_{2\nu}$)
C_{80}	12	30	7	I_h^{d}, D_{5d}, D_{5h}, $C_{2\nu}$ (2), D_3, D_2	20 (D_2)
C_{82}	12	31	9	C_2 (3), C_s (3), $C_{3\nu}$ (2), $C_{2\nu}$	41 (C_2)
C_{84}	12	32	24 (3 + 21)	C_1 to T_d	11 (D_{2d}), 21 (D_2)
C_{90}	12	35	46	C_1 (18), C_2 (14), $C_{2\nu}$ (6) and others	

[a] See figure 2 for some fullerene polyhedra that have been observed experimentally; fullerenes not observed experimentally are listed in bold.
[b] The partitioning of the IPR structures into families related by pyracylene transformations (figure 4) is given in parentheses.
[c] For fullerenes C_n ($n \geqslant 76$) only the numbers of different vertices for fullerenes observed experimentally are given.
[d] The T_d structure for C_{76} and the I_h structure for C_{80} are open shell structures.

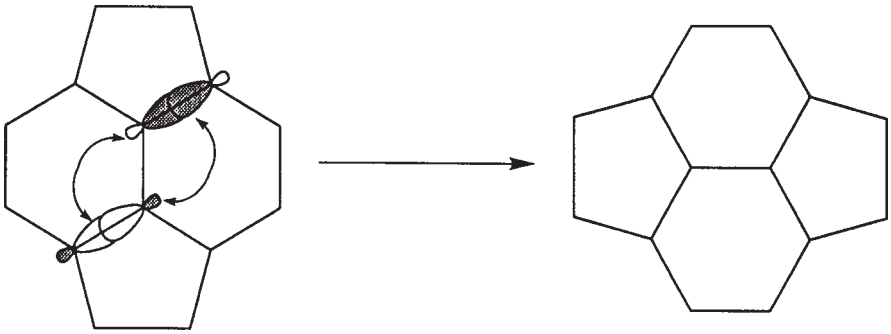

Figure 4. The pyracylene (Stone–Wales) transformation.

terconversion by the pyracylene transformation under the conditions of their synthesis in graphite arcs so that the number of isolable C_n fullerenes reflects the number of closed families of interconverting isomers.

Consider a fullerene structure consisting of a cage of sp^2 hybridized carbon atoms with different arrangements of the hexagonal and pentagonal rings. The pyracylene transformation for interchanging the positions of the hexagons and pentagons is illustrated in figure 4. The concerted shift of σ-bonds considered as a pericyclic chemical process leads to a four-electron Hückel transition state [21]. Although this process is thermally forbidden, this structural transformation can be formally applied to any of the bonds between two pentagons to generate many different species. Of particular significance in understanding the higher fullerenes are series of pyracylene transformations interconverting IPR isomers without any intermediates violating the IPR.

2.3. The leapfrog transformation

Another process for generating larger fullerenes from smaller fullerenes is the so-called *leapfrog transformation* [20]. The leapfrog transformation consists of omnicapping followed by dualization and generates a fullerene cage of $3n$ carbon atoms from any fullerene cage of n carbon atoms. In the omnicapping stage, each face of the original polyhedron is capped with an extra atom to make a local pyramid so that the resulting omnicapped polyhedron, which necessarily is a deltahedron, can be regarded as a "compound" of the original polyhedron and its dual where the dual polyhedron is generated from the apices of the local pyramids. The processes of omnicapping and dualization making up the leapfrog transformation both preserve the symmetry of the original polyhedron. Furthermore, applying the leapfrog transformation to any fullerene leads to a fullerene with a stable closed-shell electronic structure. The effects of applying a leapfrog transformation to a hexagon, a pentagon, a heptagon, a vertex, and an edge of a carbon network are depicted in figure 5. Application of a leapfrog transformation to a regular dodecahedron (i.e., the hypothetical C_{20}) to give the truncated icosahedron of the C_{60} fullerene through an omnicapped dodecahedron intermediate is depicted in figure 6. Since fullerene structures are feasible for any

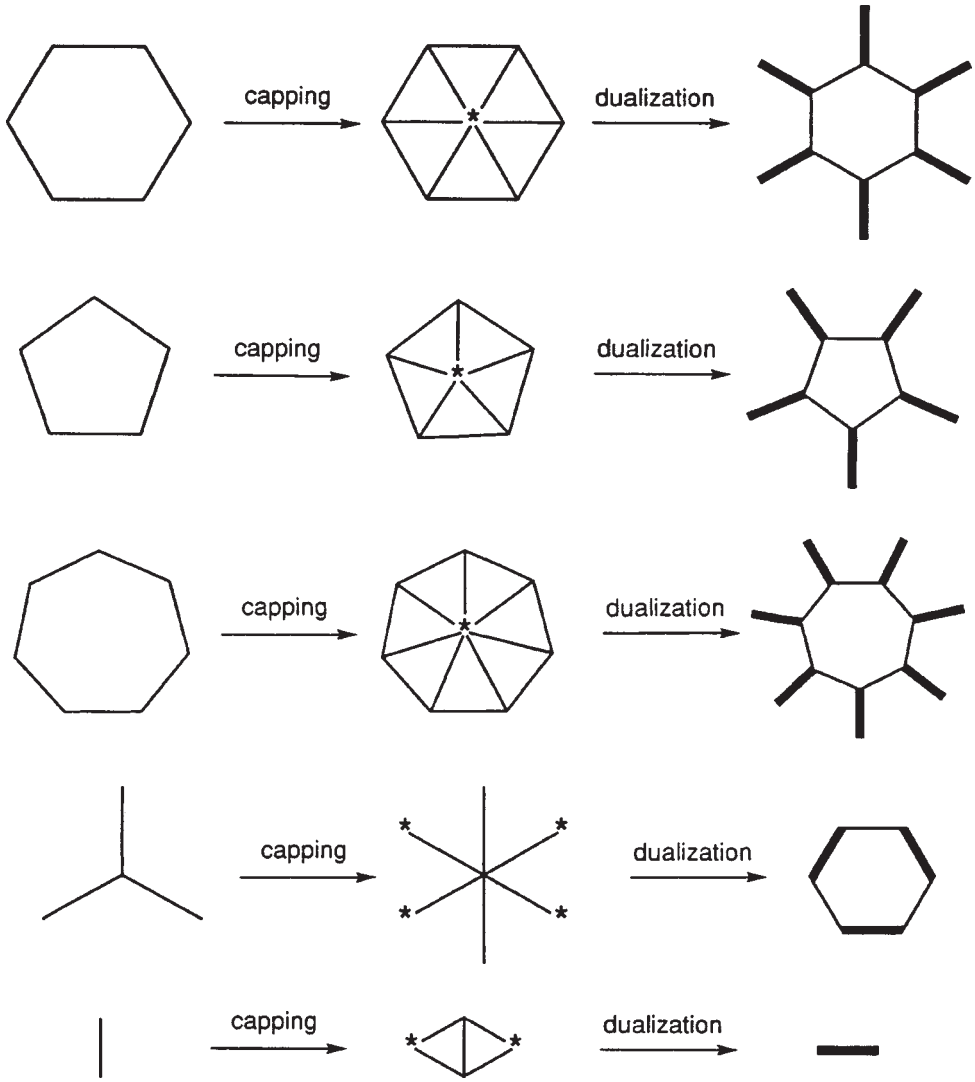

Figure 5. A schematic description of the effect of the leapfrog transformation on a hexagonal face, a pentagonal face, a heptagonal face, a vertex, and an edge. The second column shows elements of the intermediate omnicapped deltahedron and the third column their counterparts in the final leapfrog polyhedron. Double bonds in a carbon structure are shown as bold lines.

C_n cage where $n = 20 + 2k$ ($k \neq 1$), stable fullerenes generated by the leapfrog transformation occur with $60 + 6k$ ($k \neq 1$) vertices.

The rules associated with leapfrog transformations can be proven formally using bounding theorems for matrix eigenvalues [54]. However, the plausibility of such rules can be seen by noting that a double bond can be associated with every edge of the leapfrog arising from its parent and single bonds with the other edges (note the bold edges in figure 5). This arrangements of single and double bonds results in the

maximum for a C_n fullerene of $n/3$ benzenoid hexagons, each containing three double bonds [18].

2.4. *Fullerenes of icosahedral symmetry and their energy levels*

Fullerene polyhedra of the highest possible symmetry, namely icosahedral, are of particular interest as exemplified by C_{60}. Each fullerene polyhedron of icosahedral symmetry uniquely corresponds to a pair of integers h, k such that $0 < h \geqslant k \geqslant 0$ with the number of vertices T being defined by the following equation:

$$T = 20\big(h^2 + hk + k^2\big). \tag{8}$$

A fullerene satisfying equation (8) has full I_h icosahedral rotational and reflection symmetry if $k = 0$ or $h = k > 0$, but only the chiral I pure rotational symmetry if $h > k \neq 0$.

The simplest polyhedron satisfying equation (8) is the regular dodecahedron for which $h = 1$ and $k = 0$ so that $T = 20$. The truncated icosahedron found in C_{60} (figure 2) satisfies equation (8) for $h = k = 1$ and is derived from the regular dodecahedron by a single application of the leapfrog transformation as depicted in figure 6. In any fullerene polyhedron with icosahedral symmetry, the centers of the 12 pentagonal faces form a large icosahedron.

Polyhedra of icosahedral symmetry having only pentagonal and hexagonal faces in which all vertices have degree 3 and thus satisfying equation (8) are called *Goldberg polyhedra* [22]. Fowler [17] has shown that the Goldberg polyhedra for carbon clusters follow an electron-counting rule analogous to the famous Hückel $4k+2$ (k integer) rule for planar polygonal hydrocarbons. Thus when $h - k$ is divisible by three the carbon cluster has a multiple of 60 atoms and has a closed shell electronic configuration; otherwise the carbon cluster has $60m + 20$ atoms (m integer) and has an open shell electronic configuration. The smallest example of an open-shell IPR fullerene with icosahedral symmetry is the I_h C_{80} isomer listed in table 1 which follows the $60m+20$

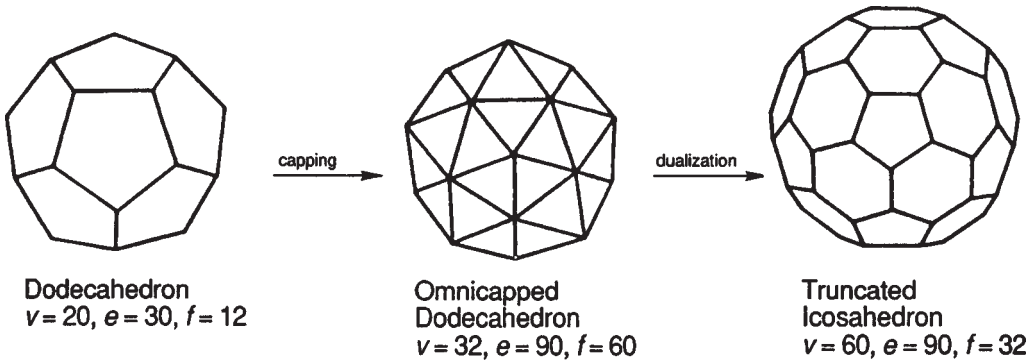

Figure 6. Application of the leapfrog transformation to the regular dodecahedron to give the truncated icosahedron of C_{60} through an omnicapped dodecahedron intermediate.

rule, where $m = 1$. If a particular value of T satisfies equation (8), then so do $3T$, $9T$, $27T$, etc. This follows from equation (8) since if equation (8) is satisfied then

$$3T = H^2 + HK + K^2, \tag{9}$$

where $H = h + 2k$ and $K = h - k$. These considerations predict stable closed-shell icosahedral fullerenes with 60, 180, 240, 420, 540, ... carbon atoms.

The molecular orbitals of the simplest fullerene of icosahedral symmetry, namely, C_{60}, are of interest because of their relationship to the superconductivity of compounds obtained by reduction of C_{60} with alkali metals [25]. For example, the A_3C_{60} phases (A = alkali metal) have been found [62] to exhibit superconductivity with T_c's around 20 K (e.g., 18 K for K_3C_{60}). These superconducting materials retain the solid state C_{60} face-centered cubic structure with slightly modified lattice constants and thus may be regarded as three-dimensional materials. More extensive reduction of C_{60} with alkali metals lead to insulating orthorhombic A_4C_{60} and insulating body-centered cubic A_6C_{60} phases.

The origin of the superconductivity in these reduced C_{60} materials can be understood by consideration of the electronic structure of C_{60} [15]. The bonding character in the C_{60} cage may be regarded as predominantly sp^2 with a small amount of sp^3 character arising from the nonzero curvature of the C_{60} surface. The approximation of the truncated icosahedron of C_{60} by a sphere suggests labeling of its electronic states in terms of spherical harmonics, in which the σ and π electrons correspond to different radial quantum numbers [10].

These spherical harmonics used to describe the molecular orbital energy levels of fullerenes of icosahedral symmetry are mathematically analogous to the functions used to describe atomic orbitals and thus arise from solution of the following well-known second-order differential equation in which the potential energy V is spherically symmetric:

$$\frac{\partial^2\Psi}{\partial x^2} + \frac{\partial^2\Psi}{\partial y^2} + \frac{\partial^2\Psi}{\partial z^2} + \frac{8\pi^2 m}{h^2}(E - V)\Psi = \nabla^2\Psi + \frac{8\pi^2 m}{h^2}(E - V)\Psi = 0. \tag{10}$$

The resulting wave functions, Ψ, may be factored into the product

$$\Psi(r, \theta, \phi) = R(r)\Theta(\theta)\Phi(\phi), \tag{11}$$

in which the factors R, Θ and Φ are functions solely of r, θ and ϕ, respectively, which are related to the Cartesian coordinates x, y and z by the following equations:

$$x = r \sin\theta \cos\phi, \tag{12a}$$

$$y = r \sin\theta \sin\phi, \tag{12b}$$

$$z = r \cos\theta. \tag{12c}$$

Since the value of the radial component $R(r)$ of Ψ is completely independent of the angular coordinates θ and ϕ, it is independent of direction (i.e., *isotropic*) and therefore remains unaltered by any symmetry operations. For this reason all of the symmetry

properties of a spherical harmonic Ψ are contained in its angular component $\Theta(\theta)\Phi(\phi)$ which is defined by the scalar spherical harmonics $Y_{lm}(\theta, \phi)$, i.e.,

$$\Theta(\theta)\Phi(\phi) = Y_{lm}(\theta, \phi). \tag{13}$$

Each of the three factors of Ψ (equation (11)) generates a quantum number. Thus the factors $R(r)$, $\Theta(\theta)$ and $\Phi(\phi)$ generate the quantum numbers N, L and M, respectively. The *principal quantum number* N, derived from the radial component $R(r)$, relates to the distance from the center of the sphere (i.e., the nucleus in the case of atomic orbitals). The *azimuthal quantum number* L, derived from the factor $\Theta(\theta)$ in equation (11), relates to the number of nodes in the angular component $\Theta(\theta)\Phi(\phi)$, where a *node* is a plane corresponding to a zero value of $\Theta(\theta)\Phi(\phi)$ or Ψ, i.e., where the sign of $\Theta(\theta)\Phi(\phi)$ changes from positive to negative. Molecular orbitals of spherical molecules where $L = 0$, 1, 2, 3, 4, 5, etc. are conventionally designated as S, P, D, F, G, H, etc. orbitals, respectively, by analogy with standard designations of atomic orbitals and their quantum numbers but using capital letters. For a given value of the azimuthal quantum number L, the *magnetic quantum number* M, derived from the factor $\Phi(\phi)$ in equation (11), indicates the tilt of the plane of orbital motion with respect to some reference direction [34] (typically, the z-axis) and may take on all $2L + 1$ different values from $+L$ to $-L$. There are therefore necessarily $2L + 1$ distinct orthogonal orbitals for a given value of L corresponding to 1, 3, 5, 7, 9 and 11 distinct S, P, D, F, G and H orbitals, respectively. Thus a set of molecular orbital energy parameters satisfactorily approximated by spherical harmonics must be partitioned into relatively closely spaced groups of 1, 3, 5, 7, 9, etc. molecular orbitals starting with the molecular orbital of lowest energy corresponding to the highest eigenvalue of the corresponding graph.

The use of spherical harmonics in a Hückel theory based approach to describe the molecular orbitals of C_{60} is closely related to the tensor surface harmonic methods of Stone [63–66], which have been applied to deltahedral boranes by using spheres to approximate borane deltahedra. The bonding σ-states of C_{60} relate to edge-localized σ-bonds along the 90 edges of the truncated icosahedron and reside well below the highest occupied molecular orbital (HOMO) of C_{60}, which is composed of orbitals having primarily π character. The resulting molecular orbital energy levels of C_{60} based on this spherical harmonic analogy using the terminology of Stone [63–66] as well as standard molecular orbital terminology to label the energy levels are depicted in figure 7. The 25 molecular orbitals labeled S, P, D, F and G corresponding to the values 0, 1, 2, 3 and 4, respectively, for the spherical quantum number l are filled with 50 of the 60 π electrons of C_{60} leaving 10 electrons to occupy part of the H molecular orbital, which is split by the icosahedral symmetry of C_{60} into a five-fold degenerate h_u HOMO, a three-fold degenerate lowest unoccupied t_{1u} molecular orbital (LUMO), and an additional three-fold degenerate level of slightly higher energy. In C_{60} the ten H π-electrons fill exactly the fivefold h_u level giving a closed-shell configuration (figure 7).

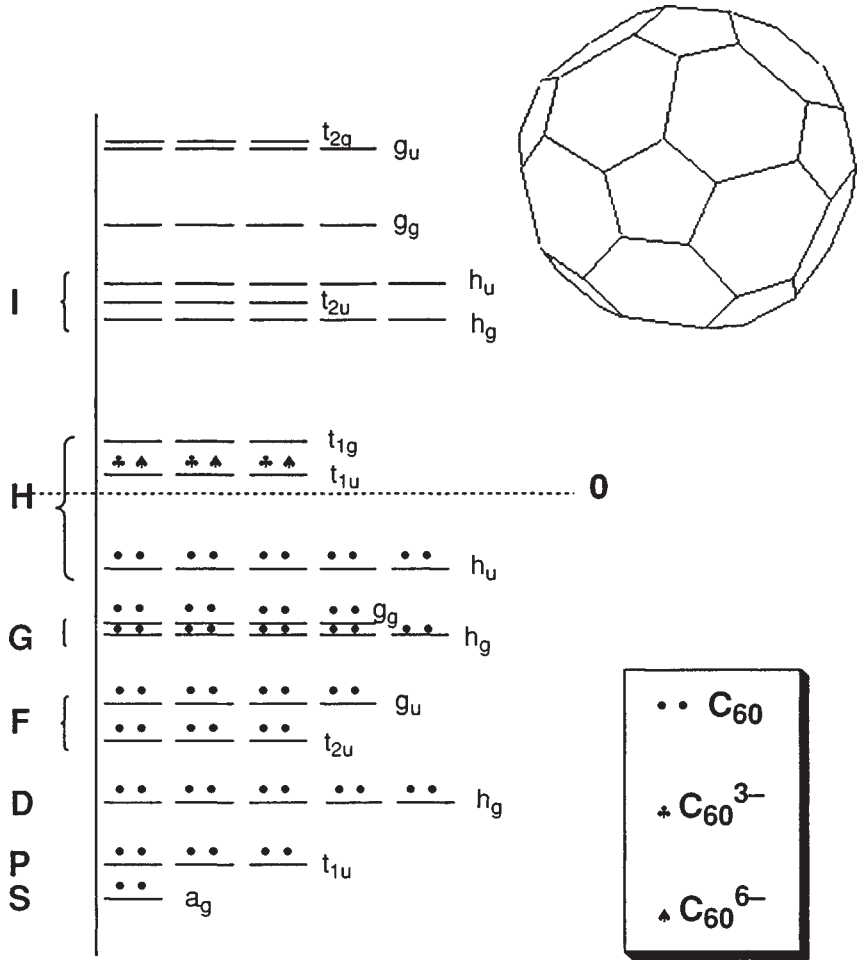

Figure 7. The spherical harmonic structure of the molecular orbital energy levels of C_{60}. The 60 electrons for neutral C_{60} are indicated by •. The additional 3 electrons of C_{60}^{3-} and the additional 6 electrons of C_{60}^{3-} in the t_{1u} molecular orbital are indicated by ♣ and by ♣ + ♠, respectively.

Electronic band theory based on the molecular orbital energy levels of C_{60} in figure 7 provides a consistent explanation of the electrical properties of C_{60}-derived materials. Both neutral C_{60} (• in figure 7) and the hexaanion C_{60}^{6-} found in K_6C_{60} (• + ♣ + ♠ in figure 7) exhibit semiconducting properties in accord with their closed shell configurations whereas the trianion C_{60}^{3-} found in K_3C_{60} (• + ♣ in figure 7) has a partially filled HOMO corresponding to a Fermi surface and leading to metallic properties. The C_{60}^{3-} salts of relatively compact cations such as K^+ are not only metallic but exhibit superconductivity with T_c's up to 18 K for K_3C_{60} [62].

Tang et al. [68] have performed Hückel calculations on the first four members of the C_{60n^2} series ($1 \leqslant n \leqslant 4$) of spherical fullerenes of icosahedral symmetry. Their calculations provide sets of molecular orbital energy parameters whose approximation

by spherical harmonics can be analyzed. This provides some insight as to the relationship of the large icosahedrally symmetric structures of the C_{60n^2} fullerenes to ideal spheres.

The following general observations can be made from the calculations of Tang et al. [68] concerning the distribution of the energy parameters of the bonding molecular orbitals of the icosahedral C_{60n^2} fullerenes ($0 < n \leqslant 4$):

(1) The most positive eigenvalue is always exactly $+3$ in accord with the fact that all vertices of any fullerene polyhedron has degree 3.

(2) Fullerene polyhedra are clearly not bipartite graphs because of the presence of the 12 pentagonal faces. For this reason the eigenvalues of the corresponding graph spectra cannot be grouped into $\pm x_i$ pairs. Nevertheless, the C_{60n^2} fullerenes of icosahedral symmetry have equal numbers of bonding and antibonding orbitals as well as a high HOMO/LUMO separation. For this reason neutral C_{60n^2} fullerenes of icosahedral symmetry are expected to be stable [3].

(3) There are five types of irreducible representations of the icosahedral rotation group I, namely, A, T_1, T_2, G and H representations of degeneracies 1, 3, 3, 4 and 5, respectively. Therefore the observed molecular orbitals exhibit these degeneracies except for the much larger accidental degeneracies at the $+1$ eigenvalue of 9, 10, 9 and 30 for C_{60}, C_{240}, C_{540} and C_{960}, respectively [68]. The HOMO and LUMO for any of these C_{60n^2} fullerenes of icosahedral symmetry are quintuply degenerate h and triply degenerate t_1 orbitals, respectively. The entire set of $60n^2$ molecular orbitals for C_{60n^2} can be partitioned into $n^2(a + 3t_1 + 3t_2 + 4g + 5h)$ sets so that the total number of *distinct* energy levels is $16n^2$.

(4) From the most positive $+3$ eigenvalue to the highly degenerate $+1$ eigenvalue the molecular orbitals are clustered into groups of 1, 3, 5, 7, 9, ... orbitals as expected for the S, P, D, F, G, H, ... spherical harmonics corresponding to $L = 0$, 1, 2, 3, 4, 5, ..., respectively. Thus the lowest lying molecular orbitals (i.e., the molecular orbital with a $+3$ eigenvalue) is always a non-degenerate a orbital ($L = 0$) followed by triply degenerate t_1 and quintuply degenerate h orbitals for $L = 1$ and 2, respectively.

The lowest lying molecular orbitals of C_{60} (figure 7) are grouped into sets of 1, 3, 5 and 7 molecular orbitals of alternating parity g, u, g and u as expected for S, P, D and F molecular orbitals derived from spherical harmonics with $L = 0$, 1, 2 and 3, respectively. Next at the $+1$ eigenvalue come the accidentally nine-fold degenerate ($g_g + h_g$) G orbitals of the expected gerade (g) parity. These G orbitals are followed by a group of 11 orbitals divided into an ($h_u + t_{1u} + t_{1g}$) set which are the frontier orbitals since they bracket the zero eigenvalue separating bonding and non-bonding orbitals. Although the number of these orbitals is correct for the expected 11 H orbitals, the parities are wrong since all true H orbitals would be expected to be ungerade. Thus the molecular orbitals of C_{60} are no longer adequately approximated by spherical harmonics in the frontier orbital range.

Figure 8 depicts the bonding molecular orbitals of C_{240} as calculated by Tang et al. [68]. These molecular orbitals are grouped into clusters of 1, 3, 5, 7, 9, 11, 13, 15

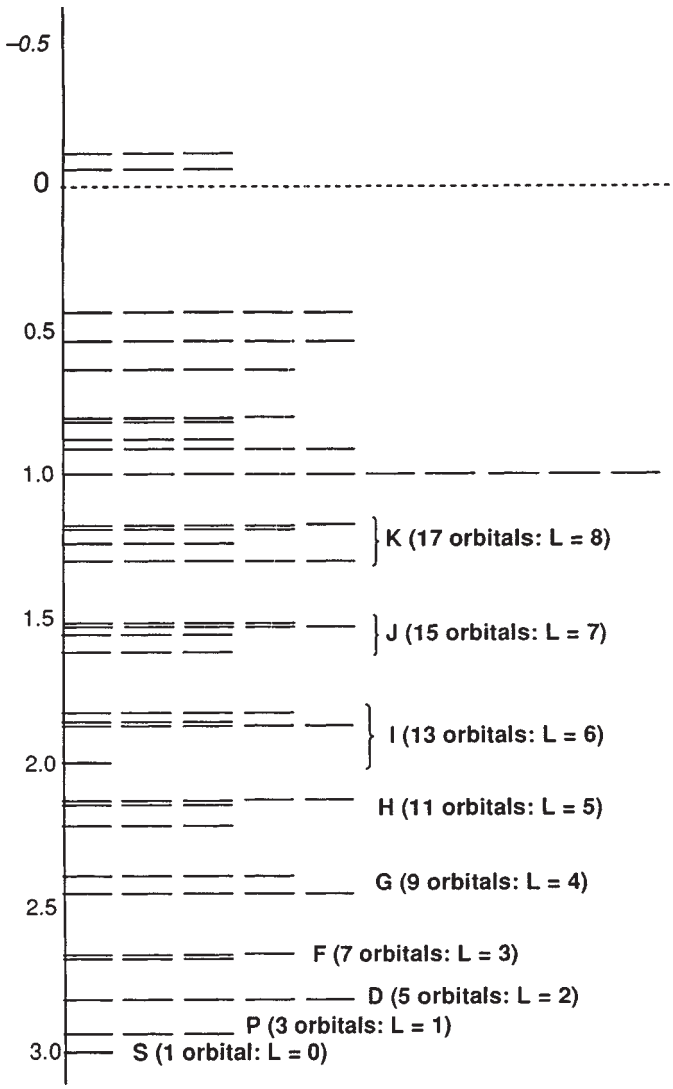

Figure 8. The spherical harmonic structure of the bonding molecular orbital energy levels of C_{240}.

and 17 orbitals as expected for molecular orbitals derived from spherical harmonics with $L \leqslant 8$. This pattern breaks down at and beyond the 10-fold degenerate $+1$ eigenvalue since immediately beyond the 17 orbitals with $L = 8$ it is not possible to segregate a group of 19 orbitals for $L = 9$. This suggests that the spherical harmonic approximation for the molecular orbitals of C_{240} breaks down for molecular orbitals with eigenvalues $+1$ and beyond (i.e., *below* $+1$ since the lowest lying molecular orbital is always at $+3$).

Similar methods can be used to analyze the molecular orbitals of the higher C_{60n^2} fullerenes of icosahedral symmetry [36].

3. Schwarzites: hypothetical negative curvature polymeric carbon allotropes

3.1. A proposed "fourth form of carbon"

Analysis of the structures of graphite and fullerenes suggests a fourth form of elemental carbon based on networks of trigonal sp^2 carbon atoms decorating surfaces of negative rather than positive curvature. The negative curvature surfaces of interest are called infinite periodic minimal surfaces (IPMS's) and are expected to lead to polymeric carbon allotropes having unusually low density. Since the relevant negative curvature surfaces were first studied in detail by the mathematician H.A. Schwarz in 1880 [61], the trivial name *schwarzite* has been suggested for this still unknown form of carbon [50]. The carbon rings on the negative curvature surfaces of schwarzite structures are expected to include heptagons and/or octagons in addition to an indeterminate number of hexagons. The carbon heptagons and octagons introduce negative curvature into the schwarzite surfaces.

Mackay and Terrones appear to have been the first to recognize the possibility of negative curvature allotropes of carbon and in 1991 [52] they proposed the P192 schwarzite structure with a unit cell of 192 carbon atoms in a simple cubic structure based on the IPMS called the P surface. Their proposed schwarzite structure was quickly followed by the 216 atom unit cell P216 and D216 schwarzite structures of Lenosky et al. [50] based on the P and D surfaces, respectively, and the 168 atom unit cell D168 schwarzite structure of Vanderbilt and Tersoff [69] also based on the D surface. Subsequently, schwarzite structures having only one type of carbon atom in a 24-atom unit cell were studied by O'Keeffe et al. [57].

The smallest stable pure carbon fullerene structure is C_{60} (figure 2), which is the smallest fullerene structure containing enough carbon hexagons so that no pair of the 12 pentagonal faces needs to share any edges. The higher stable fullerenes, namely, C_n ($n = 70$ and higher even numbers), have a large number of carbon hexagons separating the 12 pentagonal faces with C_{70} (figure 2) being the second smallest possible fullerene obeying the IPR.

Similar ideas can be used to analyze possible schwarzite structures. For example, Vanderbilt and Tersoff [69] construct their D168 schwarzite structure by giving each carbon vertex a "perfect local topology" similar to that of the carbon vertices in the C_{60} fullerene. Thus in C_{60} each carbon vertex is shared by one pentagon and two hexagons, each pentagon is surrounded by only hexagons, and each hexagon is surrounded by alternating hexagons and pentagons. The D168 schwarzite structure of Vanderbilt and Tersoff [69] has an analogous local carbon vertex topology with each vertex being shared by one heptagon and two hexagons, each heptagon being surrounded by only hexagons, and each hexagon being surrounded by alternating hexagons and heptagons.

A striking feature of the C_{60} structure (figure 2) is its high symmetry based on the icosahedral pure rotation group of order 60 (the I group), which is the largest finite three-dimensional rotation point group having relatively small order rotation axes. If the concept of symmetry in carbon allotrope structures is broadened to include

automorphism groups containing permutations other than standard symmetry operations, then the D168 schwarzite structure proposed by Vanderbilt and Tersoff [69] can also be seen to have unusually high permutational symmetry with an automorphism group of order 168, conventionally designated as PSL(2,7) [35]. The PSL(2,7) group in question has been known since the 19th century as a transitive permutation group on either seven or eight objects just like the icosahedral rotation group is a transitive permutation group on either five or six objects [23]. This analogy between these unusual symmetries of the C_{60} fullerene and the D168 schwarzite suggests the following [35]:

(1) The D168 schwarzite is the negative curvature analogue of the C_{60} fullerene.

(2) Schwarzites with larger unit cells (e.g., P192, D192 and P216) are analogues of C_{70} and higher fullerenes, which, in general, are less symmetrical than C_{60} and have a larger number of hexagonal faces relative to the 12 pentagonal faces required by topology.

3.2. Carbon networks on surfaces of non-zero genus

Consider a network of sp^2 carbon atoms in which ν is the number of carbon atoms (vertices), e is the number of carbon–carbon bonds (edges), and f is the number of carbon rings (faces) embedded into a surface of genus g, namely, a surface homeomorphic to a sphere with g handles [53]. Thus a sphere has genus 0 and a torus or a coffee cup with a handle has genus 1. A generalized version of Euler's theorem can then be written as

$$\nu - e + f = 2 - 2g = \chi, \tag{14}$$

where χ is the *Euler characteristic*. Now consider a network of sp^2 carbon atoms containing only hexagons and heptagons so that

$$2e = 3\nu = 6f_6 + 7f_7. \tag{15}$$

Substituting this into Euler's equation gives

$$-f_7 = 12(1 - g) = 6\chi. \tag{16}$$

The solutions to this equation of lowest genus are $f_7 = 12$ for $g = 2$ or $\chi = -2$, and $f_7 = 24$ for $g = 3$ or $\chi = -4$. The latter solution is the basis of the prototypical D168 schwarzite structure [69] analogous to the C_{60} fullerene structure. The D168 structure is obtained by subjecting a fundamental structural unit of 24 heptagons embedded in a surface of genus 3 to a leapfrog transformation (figure 5). Such a unit of 24 heptagons has $24(7/3) = 56$ vertices since each heptagon has seven vertices and each vertex is shared by three heptagons. Applying the leapfrog transformation triples the 56 vertices of the fundamental structural unit to give the 168 vertices of the D168 unit cell.

3.3. *Infinite minimal periodic surfaces for negative curvature carbon allotropes*

The above analysis suggests that the unit cell of the prototypical D168 schwarzite structure can be generated by embedding 24 heptagons on a surface of genus 3. Suitable surfaces of genus 3 turn out to be infinite minimal surfaces with negative Gaussian curvature [1]. Thus, consider a curved surface, such as one formed by a network of sp^2-hybridized carbon atoms. At each point such a curved surface has two principal curvatures k_1 and k_2. The mean curvature H and the Gaussian curvature K are defined as follows:

$$H = \frac{1}{2}(k_1 + k_2), \tag{17a}$$

$$K = k_1 k_2. \tag{17b}$$

A spherical or ellipsoidal shell has positive Gaussian curvature (i.e., it is "convex"), a hyperbolic sheet has negative Gaussian curvature (i.e., it is "concave"), and a cylinder or cone has zero Gaussian curvature. Minimal surfaces are surfaces where the mean curvature H at each point is zero so that $k_1 = -k_2$ by equation (17a) and $K \leqslant 0$ by equation (17b). They are thus saddle-shaped everywhere except at certain "flat points" which are higher order saddles. The simplest example of a (non-periodic) minimal surface excluding the trivial case of the plane is defined by the following cubic equation:

$$F(x, y) = z = x\big(x^2 - 3y^2\big). \tag{18}$$

This surface (figure 9(a)) is called the *monkey saddle* [27], since it has three depressions, namely two for the monkey's legs and one for his tail. The average curvature of the monkey saddle vanishes at every point so that at every point its "concavity" is equal to its "convexity".

It is not possible to construct an infinite surface with a *constant* negative Gaussian curvature. However, Schwarz found before 1865 that patches of *varying* negative curvature and constant zero mean curvature could be smoothly joined to give an infinite surface with zero mean curvature which is periodic in all three directions. Such surfaces are called infinite periodic minimal surfaces (IPMS's). About five different types of IPMS's were known by 1880 [56] and the number of known distinct IPMS's is now more than 50 [16]. The original five IPMS's have been given the designations P, D, T, H and CLP and have been depicted as polyhedral wire models dipped into soap solutions which correspond to their unit cells (table 2) [1]. These IPMS's can be constructed using monkey saddles (figure 9(a)) as basic building blocks so that the single flat point of each monkey saddle is located at a vertex of the polyhedral unit cell.

The IPMS's described above cannot be defined by analytic functions in the usual Cartesian space of three dimensions but instead requires elliptic or hyperelliptic integrals, which must be solved numerically [1]. The finite surface element building block

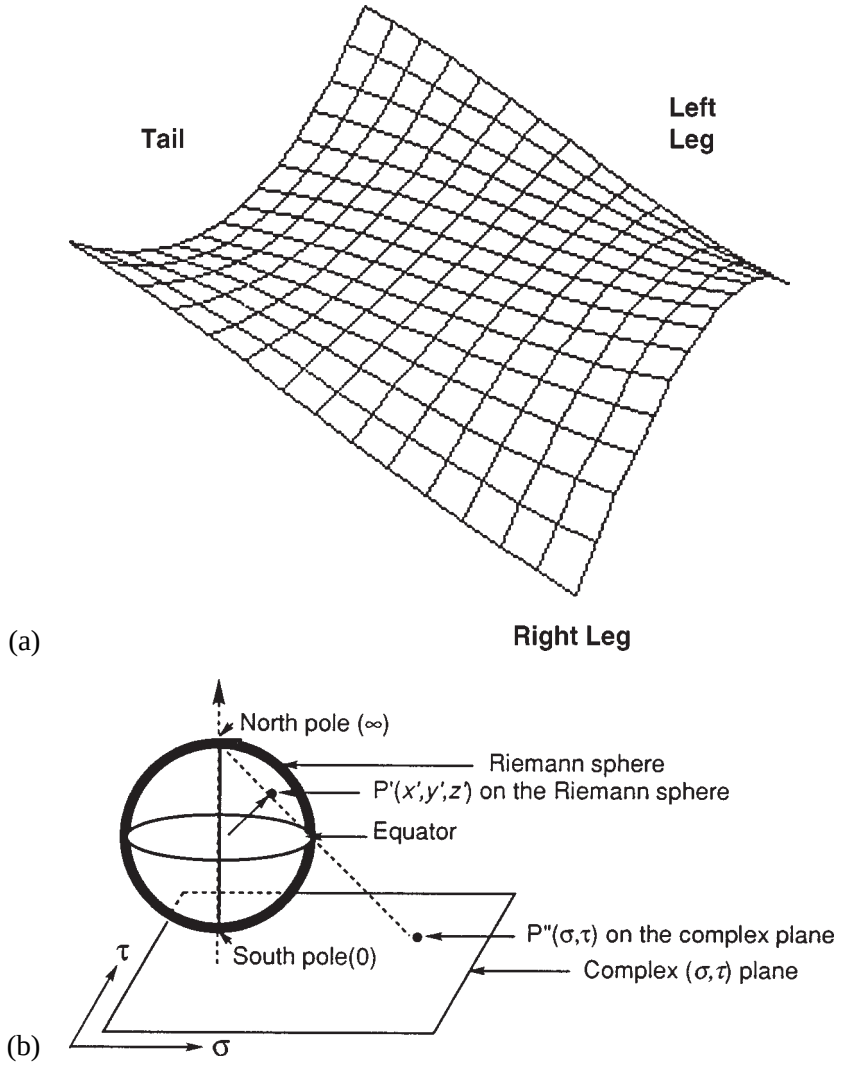

Figure 9. (a) The monkey saddle as defined by equation (18); (b) The Riemann sphere and the projection of a point $P'(x', y', z')$ on the Riemann sphere to a point $P''(\sigma, \tau)$ in the complex plane.

Table 2
Polyhedral unit cells for the five classical minimal surfaces.

Surface	Genus	Polyhedron	Symmetry	Number of edges
P	3	Octahedron	O_h	6 out of 12
D	3	Tetrahedron	T_d	4 out of 6
T	3	Cube	O_h	8 out of 12
CLP	3	Trigonal prism	D_{3h}	
H	3	Triangle	D_{3h}	3 out of 3

which is repeated periodically throughout space in an IPMS plays a role analogous to the unit cell in a crystal structure. Hyde and collaborators have exploited this analogy to describe crystal structures using IPMS's [1,2,28–31].

The description of IPMS's using elliptic or hyperelliptic integrals is facilitated by the fact that minimal surfaces are the only surfaces other than the sphere whose spherical representation is conformal. This means that every complex analytic function can be used to describe a minimal surface. In order to generate such a description, each point $P(x, y, z)$ of the surface is mapped onto a point $P'(x', y', z')$ on the unit sphere given by

$$P'(x', y', z') = \frac{(\mathrm{d}F/\mathrm{d}x, \mathrm{d}F/\mathrm{d}y, \mathrm{d}F/\mathrm{d}z)}{\sqrt{(\mathrm{d}F/\mathrm{d}x)^2 + (\mathrm{d}F/\mathrm{d}y)^2 + (\mathrm{d}F/\mathrm{d}z)^2}}. \tag{19}$$

The same sphere, taken as a special unit sphere called the *Riemann sphere*, can also be used to represent the complex numbers $\omega = \sigma + \mathrm{i}\tau$ by points on the (σ, τ) complex plane (figure 9(b)). The complex plane can correspond to the equatorial plane of the Riemann sphere (figure 9(b)) in which the north pole is ∞ and the south pole is 0; the $0{-}\infty$ axis can be called the *polar axis* [40]. In this way the point $P'(x', y', z')$ on the Riemann sphere can be projected to the point $P''(\sigma, \tau)$ on the complex plane (figure 9(b)). Weierstrass showed in the 19th century that the Cartesian coordinates of a point $P(x, y, z)$ on an IPMS are related to the coordinates $P''(\sigma, \tau)$ on the complex plane by the integrals

$$x = \mathrm{Re} \int \left(1 - \omega^2\right) R(\omega)\, \mathrm{d}\omega, \tag{20a}$$

$$y = -\,\mathrm{Im} \int \left(1 + \omega^2\right) R(\omega)\, \mathrm{d}\omega, \tag{20b}$$

$$z = \mathrm{Re} \int 2\omega R(\omega)\, \mathrm{d}\omega, \tag{20c}$$

in which Re and Im denote the real and imaginary parts of the complex integral and $\omega = \sigma + \mathrm{i}\tau$ as above.

The Weierstrass function $R(\omega)$ determines the intrinsic parameters of the surface. For example, the Gaussian curvature is related to $R(\omega)$ by the following equation:

$$K = \frac{-4}{(1 + |\omega|^2)^4 |R(\omega)|^2}. \tag{21}$$

The general form of the Weierstrass function can be expressed as

$$R(\omega) = \frac{1}{(F(\omega))^{1/b}} = \frac{1}{\prod_{i=1}^{k} (\omega - \omega_i)^{1/b}}, \tag{22}$$

in which $k = 8$ and $b = 2$ for the IPMS's of greatest interest. The integrals in equations (20) are hyperelliptic integrals if $b = 2$ in equation (22) and the degree of the polynomial $F(\omega)$ is greater than four. The values of the roots ω_i of the polynomial

$F(\omega)$ correspond to the locations of the singular flat points of the monkey saddles making up the IPMS.

Table 2 lists the five classical IPMS's. Among these five IPMS's, two of them, namely the D and P surfaces, have the same Weierstrass function, namely,

$$R(\omega) = \frac{1}{\sqrt{1 - 14\omega^4 + \omega^8}}. \tag{23}$$

The integrals (equations (20)) determining the coordinates of these surfaces are hyperelliptic integrals since the degree of the polynomial in ω under the radical sign in equation (23) is greater than four. Furthermore, the locations of the eight roots of the degree 8 polynomial in the denominator of equation (23) correspond to the vertices of a cube inscribed in the Riemann sphere in accord with the cubic symmetry of the unit cell of the D and P surfaces. Polynomials of this type, which vanish at the vertices of a regular polyhedron inscribed in the Riemann sphere, are called *polyhedral polynomials* and have been studied for the regular polyhedra, particularly in connection with the solution of the general quintic equation using elliptic functions [12,33,37,40].

The transformation, defined by the coordinates

$$x = \mathrm{Re} \int \mathrm{e}^{\mathrm{i}\theta} \left(1 - \omega^2\right) R(\omega)\, \mathrm{d}\omega, \tag{24a}$$

$$y = -\,\mathrm{Im} \int \mathrm{e}^{\mathrm{i}\theta} \left(1 + \omega^2\right) R(\omega)\, \mathrm{d}\omega, \tag{24b}$$

$$z = \mathrm{Re} \int \mathrm{e}^{\mathrm{i}\theta} 2\omega R(\omega)\, \mathrm{d}\omega, \tag{24c}$$

is used to relate IPMS's which have the same Weierstrass function $R(\omega)$. This transformation is called a *Bonnet transformation* and the angle θ is called the *association parameter*. Surfaces related by a Bonnet transformation are called *associate surfaces*. All associate surfaces have the same metrics so that lengths are preserved during any Bonnet transformation. Thus a Bonnet transformation only bends the surface without stretching. The P and D surfaces are special cases of associate surfaces since the Bonnet transformations converting either the P to the D surface or vice versa both have $\theta = \pi/2$. Surfaces related by Bonnet transformations having $\theta = \pi/2$ are called *adjoint surfaces*.

The use of IPMS's to construct possible schwarzite structures by decorating them with networks of sp^2 carbon atoms requires consideration of their genus. In this connection all of the classical IPMS's (table 2), including the P and D surfaces suggested for schwarzite structures, are found to have unit cells with genus 3. The unit cell of the P surface is depicted in two different ways in figure 10. Thus it can be viewed as an octahedral junction of six pipes or tubes that has been called a "plumber's nightmare" (figure 10(a)) or equivalently as three hyperboloids whose axes meet at right angles (figure 10(b)). Connecting the open pipes emerging from each of the three pairs of *cis* (i.e., adjacent) faces of the plumber's nightmare (figure 10(a)) thereby generating

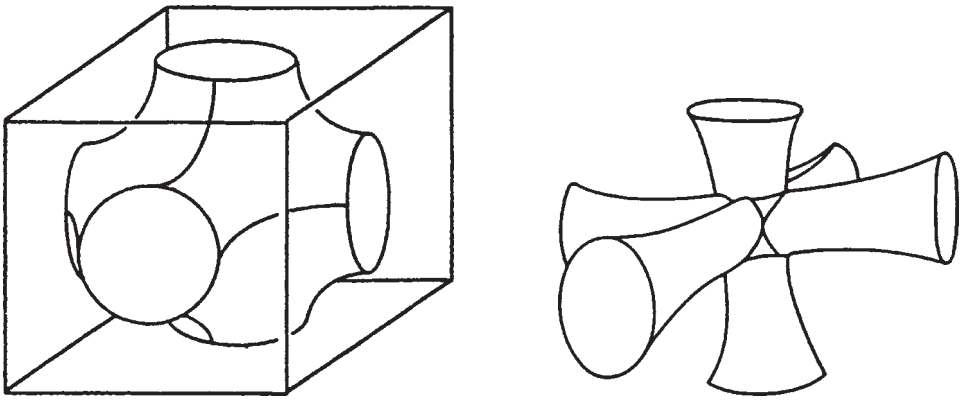

Figure 10. Two descriptions of the unit cell of the P surface: (a) A "plumber's nightmare" intersection of six pipes coming through the faces of a cube to meet at an octahedral junction; (b) Three hyperboloids whose axes intersect at right angles.

a closed surface leads to a sphere with three handles thereby indicating that a unit cell of this surface has genus 3.

3.4. Decorating infinite periodic minimal surfaces with networks of sp^2 carbon atoms

The above analysis suggests that the unit cell of the D168 schwarzite structure can be generated by decorating the unit cell of a D surface of genus 3 with 24 heptagons followed by a leapfrog transformation (figure 5) similar to the generation of the C_{60} fullerene structure by decorating a sphere with 12 pentagons to give the regular dodecahedron followed by an analogous leapfrog transformation. The D surface as well as the adjoint P surface decorated with 24 heptagons can be obtained from a figure described by the famous 19th century German mathematician F. Klein in an 1879 paper [39,41]. Figure 11, which is adapted from a figure in the 1879 Klein paper, depicts schematically an open network consisting only of full heptagons or portions thereof which can be folded to decorate a genus 3 negative curvature surface, such as a unit cell of the D or P surfaces, in the most symmetrical manner with 24 heptagons. The seven-fold symmetry (i.e., a C_7 axis) of the unfolded Klein figure (figure 11) is clearly evident in a "central" heptagon (heptagon 1) surrounded by seven additional heptagons (heptagons 2–8). An "outer group" of an additional seven heptagons (heptagons 9–15) preserves the seven-fold symmetry of this open network.

The open network of heptagons as depicted in figure 11 contains 14 outer edges, which appear as arcs because of the negative curvature of the surface. These outer edges are labeled in pairs by the letters A–G. Joining the seven pairs of outer edges labeled by the same letters generates the genus 3 surface which is topologically homeomorphic to a unit cell of the P surface and completes the remaining nine of the total of 24 heptagons by joining their pieces found in regions which are separated in the orig-

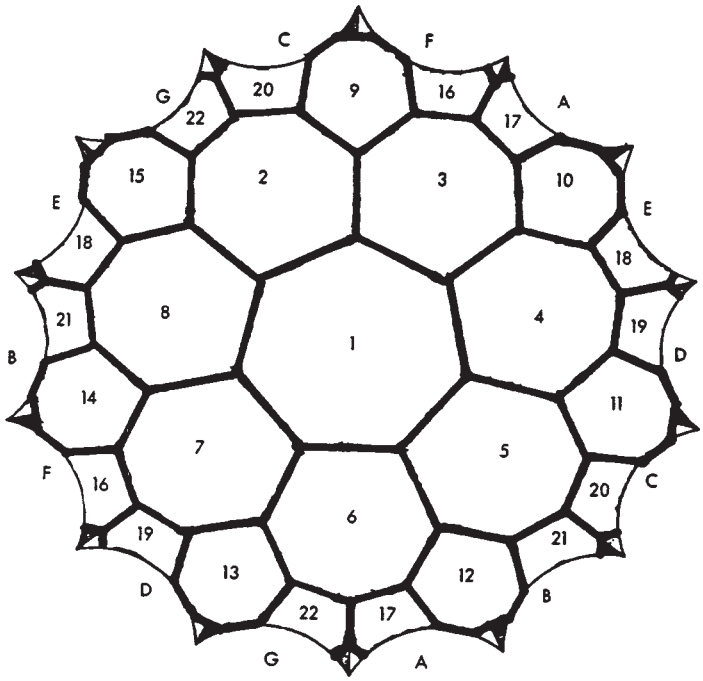

Figure 11. The figure of 24 heptagons described by Klein in his 1879 paper. All but two of the heptagons are numbered (1–22). Pairs of outer edges to be joined to form a genus 3 surfaces are indicated by the letters A–G.

inal open network (figure 11). Thus, heptagons 16–22 are generated by joining their halves whereas heptagons 23 and 24 (not labeled in figure 11) are each obtained by joining seven of the pieces which are the 14 "points" of the open network in figure 11 not allocated to heptagons (heptagons 1–15) or heptagon halves (heptagons 16–22). Converting the open network in figure 11 to a genus 3 surface by joining the pairs of outer edges AA through GG destroys the seven-fold rotation axis in the symmetry point group of the resulting surface but in the most symmetrical presentation increases the remaining symmetry to the octahedral symmetry of the cubic unit cell of the P surface.

Klein in his 1879 paper [39,41] also considers the most symmetrical presentation of the genus 3 figure of 24 heptagons. A cubic unit cell of the P surface (e.g., figure 10(a)) can be decomposed into eight hyperbolic triangular regions corresponding to the eight vertices of the cube. These regions may also be considered to be the eight (curved triangular) faces of a regular hyperbolic octahedron dual to the cubic unit cell. Each face contains $24/8 = 3$ of the 24 heptagons with the vertices common to the eight triplets of heptagons corresponding to the eight vertices of the underlying cube. One of these triplets of heptagons is depicted in figure 12. Each heptagon is divided into seven shaded and seven unshaded triangles for clarity. This decoration of a unit cell of the P surface with 24 heptagons has $7 \times 24/2 = 84$ edges and $7 \times 24/3 = 56$

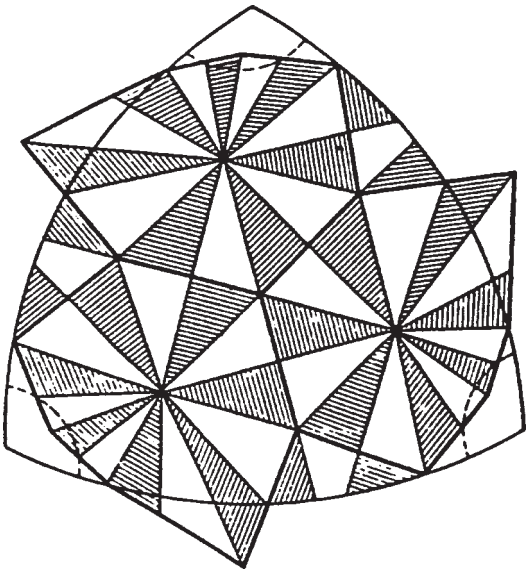

Figure 12. A triplet of heptagons contained in a hyperbolic triangular region corresponding to a face of the octahedron dual to the cube in the unit cell of the P surface. For clarity, each heptagon is divided into seven shaded and seven unshaded triangles.

vertices and thus has an Euler characteristic (equation (14)) of $56 - 84 + 24 = -4$ corresponding to genus 3. A hypothetical carbon allotrope based on this structure using the D surface, which is adjoint to the P surface, is conveniently called a D56 protoschwarzite since it has a C_{56} unit cell.

This D56 protoschwarzite structure can be converted to the D168 schwarzite structure by a leapfrog transformation (figure 5) which has the following effects:

(1) The number of vertices is increased by a factor of three giving the $3 \times 56 = 168$ vertices in the unit cell of the D168 structure.

(2) The carbon heptagons are separated by the minimum number of hexagons so that no two carbon heptagons share an edge thereby eliminating unfavorable heptalene units.

(3) The symmetry and the genus of the surface are preserved.

Table 3 compares the effects of the leapfrog transformation on the dodecahedral C_{20} fullerene and on the D56 protoschwarzite. The products of both leapfrog transformations, namely the C_{60} fullerene and the D168 schwarzite, have the following features in common:

(1) The numbers of vertices (ν) and of edges (e) belonging to non-hexagonal faces ($f_{\neq 6} + f_6$ edges in table 3) are equal (60 in the case of C_{60} and 168 in the case of D168).

Table 3
A comparison of leapfrog transformations on the C_{20} fullerene and the D56 protoschwarzite.

	$C_{20} \overset{\text{leapfrog}}{\longrightarrow} C_{60}$		D56 $\overset{\text{leapfrog}}{\longrightarrow}$ D168	
Vertices	20	60	56	168
Edges	30	90	84	252
Faces	12	32	24	80
$f_{\neq 6}$	12	12	24	24
f_6	0	20	0	56
$f_{\neq 6} + f_{\neq 6}$ edges	30	0	84	0
$f_{\neq 6} + f_6$ edges	0	60	0	168
$f_6 + f_6$ edges	0	30	0	84

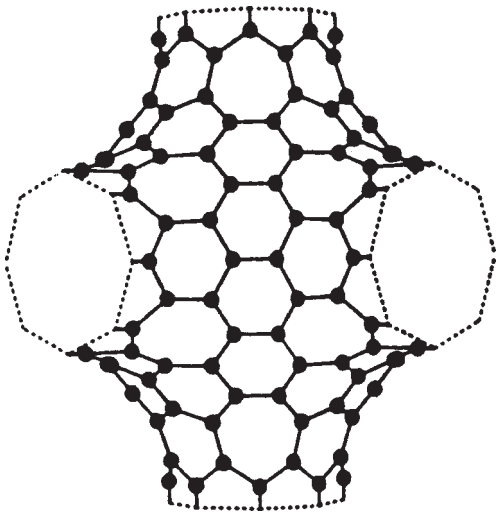

Figure 13. Placement of carbon hexagons and heptagons on a section of the P surface in the schwarzite P216.

(2) The number of edges belonging to non-hexagonal faces ($f_{\neq 6} + f_6$ edges in table 3) is twice the number of edges belonging exclusively to hexagonal faces ($f_6 + f_6$ edges in table 3).

These features suggest that the C_{60} and D168 structures both represent the minimum "dilutions" of non-hexagons with hexagons so that no pair of non-hexagons has any edges in common. For this reason C_{60} is the smallest stable fullerene. Similarly, D168 has the smallest schwarzite unit cell containing only hexagons and heptagons with no pair of heptagons having an edge in common.

Schwarzites have been suggested having unit cells with more than the minimum of 56 hexagons needed to dilute the 24 heptagons in the unit cell of a genus 3 IPMS so that no pair of heptagons has an edge in common. For example, schwarzite structures have been proposed based on the P surface with a unit cell having 216 carbon atoms,

80 hexagons, and the required 24 heptagons (figure 13) [50]. This is the schwarzite analogue of a C_{70} or larger fullerene having more than the minimum of 20 hexagons needed to dilute the 12 pentagons on a sphere so that no pair of pentagons has an edge in common.

Schwarzites have also been proposed in which the carbon rings larger than hexagons are octagons rather than heptagons. A schwarzite with only hexagonal and octagonal carbon rings based on an IPMS with a unit cell of genus 3 such as the P or D surface requires 12 octagons per unit cell. In this connection MacKay and Terrones [52] have proposed a schwarzite structure with a unit cell containing 192 carbon atoms, 80 hexagons and the required 12 octagons (table 2).

3.5. The hidden permutational symmetry of carbon allotrope structures

The structure of the C_{60} fullerene is characterized by unusually high symmetry, namely, icosahedral symmetry (i.e., the icosahedral point group I_h or its proper rotation subgroup I), which contains C_5, C_3 and C_2 proper rotation axes. A question of interest is whether the D168 schwarzite likewise has special symmetry. The cubic unit cell of D168 has O_h symmetry, which contains C_4, C_3 and C_2 axes. However, the open network of 24 heptagons (figure 11) from which the D168 structure is generated also contains a C_7 axis, which is lost from the symmetry point group when the open network is folded to a genus 3 surface by joining the outer edge pairs AA through GG. In mathematical terms [6] the open network of 24 heptagons is called a *regular map*, M, which is folded into a *polyhedral embedding* or a *polyhedral realization*, P, in a genus 3 surface. The C_7 symmetry which is "lost" when the open map (figure 11) is folded into the polyhedral embedding is called the *hidden symmetry* of the resulting polyhedral embedding [6]. This section considers a way that the C_7 symmetry element of the open 24 heptagon network can be "remembered" when the network is folded into a genus 3 surface. In order to consider the C_7 symmetry elements in the final D168 schwarzite structure, its symmetry must be considered as a permutation group of which its actual symmetry point group is a subgroup.

The description of the permutational symmetries of carbon allotrope structures requires an alternative definition of the icosahedral pure rotation group, which can be extended to larger simple permutation groups which do not occur as symmetry point groups [45]. Thus consider a prime number p and let $\mathcal{F}_p$ denote the finite field of p elements which can be represented by the p integers $0, \ldots, p-1$; larger integers can be converted to an element in this finite field by dividing by p and taking the remainder (i.e., the number is taken "mod p"). For example, the finite field $\mathcal{F}_5$ contains the five elements represented by the integers 0, 1, 2, 3 and 4, and other integers are converted to one of these five integers by dividing by 5 and taking the remainder, e.g., $6 \rightarrow 1$ in $\mathcal{F}_5$ (written frequently as "$6 \equiv 1 \bmod 5$"). The group $\mathrm{SL}(2,p)$ is defined to be the group of all 2×2 matrices with entries in $\mathcal{F}_p$ having determinant 1 and its subgroup $\mathrm{PSL}(2,p)$ for odd p is defined to be the quotient group of $\mathrm{SL}(2,p)$ modulo its center, where the center of a group is the largest normal subgroup that is Abelian. In the case

of the groups SL(2, p), where $p \geqslant 5$, the center has only two elements and the quotient group PSL(2, p) is a simple group. In this context a simple group is a group having no *normal* subgroups other than the identity group C_1, where a normal subgroup $\mathcal{N}$ of a group $\mathcal{G}$ is a subgroup which consists only of *entire* conjugacy classes of $\mathcal{G}$. The group PSL(2, 5) contains 60 elements and is isomorphic to the icosahedral pure rotation group I.

An important property of the PSL(2, p) permutation groups (table 4) for $p = 5$, 7 and 11 is that they can function as *transitive* permutation groups on sets of either p or $p + 1$ objects. In the case of the group PSL(2, 5) these transitive permutation groups on 5 and 6 objects can be visualized as permutations of parts of an icosahedron since PSL(2, 5) is isomorphic to the icosahedral pure rotation group. Thus the PSL(2, 5) group acts as a transitive permutation group on the six diameters of a regular icosahedron, where a diameter of an icosahedron is defined as a line drawn between a pair of antipodal vertices. In order to obtain in an icosahedron a set of *five* objects that is permuted transitively by the PSL(2, 5) group, the 30 edges of an icosahedron are partitioned into five sets of six edges each by the following method [40]:

(1) A straight line is drawn from the midpoint of each edge through the center of the icosahedron to the midpoint of the opposite edge.

(2) The resulting 15 straight lines are divided into five sets of three mutually perpendicular straight lines.

Each of these five sets of three mutually perpendicular straight lines resembles a set of Cartesian coordinates and defines a regular octahedron. The PSL(2, 5) permutation group as manifested in its isomorphic I symmetry point group functions as a transitive permutation group on these five sets of three mutually perpendicular straight lines. In fact the PSL(2, 5) permutation group is also isomorphic with the so-called *alternating permutation group* on five objects [38], namely, A_5, where an alternating permutation group on n objects is the set of all possible *even* permutations and is of order $n!/2$.

The next higher group in the PSL(2, p) series (table 4), namely, the PSL(2, 7) group of order 168, is important in understanding the permutational symmetry of the D168 schwarzite. In fact, the prototypical roles of C_{60} in the fullerene series and D168 in the schwarzite series relate to the fact that the number of carbon atoms in their fundamental building blocks are equal to the orders of the corresponding transitive permutation groups. Figure 14 depicts two geometrical models of the PSL(2, 7) group which reflect its dual functions as transitive permutation groups of degrees 7 and 8:

Table 4
Properties of the PSL(2, p) groups ($p = 5, 7, 11$).

Group	Order	Conjugacy classes	Polyhedral subgroup
PSL(2, 5)	60	$E + 12C_5 + 12C_5^2 + 20C_3 + 15C_2$	T
PSL(2, 7)	168	$E + 24C_7 + 24C_7^3 + 56C_3 + 21C_2 + 42C_4$	O
PSL(2, 11)	660	$E + 60C_{11} + 60C_{11}^2 + 110C_3 + 55C_2 + 132C_5 + 132C_5^2 + 110C_4$	I

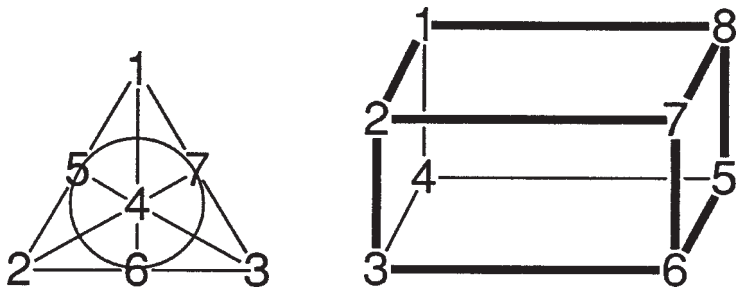

(a) D_3 7-point 7-line geometry (b) D_2 cuboid 8 points

Figure 14. Geometrical models of the PSL(2, 7) group as permutation groups on 7 and 8 points.

Degree 7 (figure 14(a)): An equilateral triangle with its three altitudes and an inscribed circle forms a 7-point 7-line geometry presented in D_3 symmetry. The permutations of the seven vertex labels which preserve the seven collineations (152, 263, 173, 146, 247, 345, 567) form the PSL(2, 7) group. Note that in this presentation the inscribed circle is treated on an equal basis with the six straight lines forming the three edges and the three altitudes of the triangle.

Degree 8 (figure 14(b)): The permutations of the eight vertex labels of a cuboid (rectangular "box") of D_2 point group symmetry (including the identity permutation) which give a set of 168 non-superimposable cuboids form the PSL(2, 7) group.

The PSL(2, p) ($p = 5, 7, 11$) groups are simple groups and thus have no non-trivial *normal* subgroups. However, they contain two different sets of n smaller subgroups corresponding to pure rotation groups of regular polyhedra (table 4); these regular polyhedral rotation groups are subgroups of index p of the groups PSL(2, p). However, the PSL(2, 11) group has been proven to the largest group of the general type PSL(2, p) with p a prime which has a subgroup of index p [45]. A corollary derived from this theorem is that if $p > 11$, the PSL(2, p) group cannot be a transitive permutation group for a set with fewer than $p + 1$ elements in contrast to the PSL(2, p) ($p = 5, 7, 11$) groups which can be transitive permutation groups for sets of p elements, namely, 5, 7 and 11, respectively.

The simplest example of the polyhedral subgroups of index p in the PSL(2, p) groups occurs in the icosahedral group PSL(2, 5), which can be decomposed into two different sets of five tetrahedra corresponding to the conjugacy classes $12C_5$ and $12C_5^2$. This is related to the partitioning of the 20 vertices of a regular dodecahedron into five sets of four vertices each corresponding to a regular tetrahedron (figure 15) [38]. The permutations of the group PSL(2, 5) act as the icosahedral pure rotation group I on the regular dodecahedron partitioned in this manner and correspondingly as the alternating group A_5 on the five subtetrahedra depicted in figure 15.

The next higher permutation group PSL(2, 7) of order 168 is highly relevant to understanding the structure and symmetry of the schwarzite D168. This group can be decomposed into two sets of seven octahedral subgroups corresponding to its conjugacy classes $24C_7$ and $24C_7^3$ (table 4). This relates to the embedding of the open

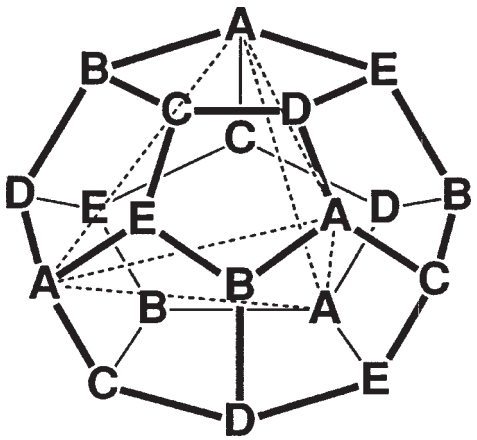

Figure 15. Partitioning the 20 vertices of a regular dodecahedron into five sets of four vertices (A–E) each corresponding to a regular tetrahedron. The six edges of tetrahedron A are indicated by dotted lines.

network (i.e., the Klein map) [33,39,41] of 24 heptagons (figure 11) into the unit cell of a P or D surface of genus 3 having a unit cell of octahedral symmetry such as the "plumber's nightmare" (figure 10). The automorphism of the Klein map (figure 11) is the PSL(2, 7) group of order 168 which thus remains the *automorphism* group of its embedding into the D surface in D168. The symmetry group of the pure rotations of the D168 unit cell is the octahedral rotation group O, which, as noted above and in table 4, is a subgroup of index 7 in PSL(2, 7). Thus the D168 schwarzite structure can be seen to have seven-fold (C_7) *hidden symmetry.*

The next higher permutation group of this type, namely PSL(2, 11) of order 660, turns out to be relevant to understanding some aspects of the symmetry of the truncated icosahedral C_{60} fullerene structure as discussed in detail in recent papers by Kostant and collaborators [8,44,45]. The PSL(2, 11) group can be decomposed into two sets of 11 icosahedral subgroups corresponding to its conjugacy classes $60C_{11}$ and $60C_{11}^2$ (table 4). In the C_{60} structure the PSL(2, 11) group acts transitively as a permutation group on the 60 vertices and the 60 edges of the 12 pentagonal faces ($f_{\neq 6} + f_6$ edges in table 3). However, the PSL(2, 11) group no longer preserves the 30 edges between two hexagonal faces ($f_6 + f_6$ edges in table 3) and therefore is not an automorphism group of C_{60}.

References

[1] S. Andersson, S.T. Hyde, K. Larsson and S. Lidin, Chem. Rev. 88 (1988) 221.
[2] S. Andersson, S.T. Hyde and H.G. von Schnering, *Z. Kristallograph.* 168 (1984) 1.
[3] D. Bakowies, M. Bühl and W. Thiel, J. Am. Chem. Soc. 117 (1995) 10 113.
[4] W.E. Billups and M.A. Ciufolini, eds., *Buckminsterfullerenes* (VCH Publishers, New York, 1993).
[5] D.A. Bochvar and E.G. Gal'pern, Dokl. Akad. Nauk SSSR 209 (1973) 610; Proc. Acad. Sci. USSR 209 (1973) 239.
[6] J. Bokowski and J.M. Wills, Math. Intelligencer 10(1) (1988) 27.

[7] E. Bruton, *Diamonds* (NAG Press, London, 1970).
[8] F. Chung, B. Kostant and S. Sternberg, in: *Lie Theory and Geometry*, eds. J.-L. Brylinski, R. Brylinski, V. Guillemin and V. Kac (Birkhäuser, Boston, 1994).
[9] J. Cioslowski, *Electronic Structure Calculations on Fullerenes and Their Derivatives* (Oxford University Press, New York, 1995).
[10] M.L. Cohen and V.H. Crespi, in: *Buckminsterfullerenes*, eds. W.E. Billups and M.A. Ciufolini (VCH Publishers, New York, 1993) pp. 197–200.
[11] R.A. Davidson, Theoret. Chim. Acta 58 (1981) 193.
[12] L.E. Dickson, *Modern Algebraic Theories* (Sanborn, Chicago, 1930) chapter XIII.
[13] F. Diederich and R.L. Whetten, Acc. Chem. Res. 25 (1992) 119.
[14] F. Diederich, R.L. Whetten, C. Thilgen, R. Ettl, I. Chao and M. Alvarez, Science 254 (1991) 1768.
[15] V. Elser and R.C. Haddon, Nature 325 (1987) 792.
[16] W. Fischer and E. Koch, Acta Cryst. A 45 (1989) 166, 169, 485, 558, 726.
[17] P.W. Fowler, Chem. Phys. Lett. 131 (1986) 444.
[18] P.W. Fowler, J. Chem. Soc. Perkin II (1992) 145.
[19] P.W. Fowler, D.E. Manolopoulos and R.P. Ryan, Chem. Comm. (1992) 408.
[20] P.W. Fowler and D.B. Redmond, Theoret. Chim. Acta 83 (1992) 367.
[21] T.L. Gilchrist and R.C. Storr, *Organic Chemical Reactions and Orbital Symmetry* (Cambridge University Press, Cambridge, 1972) p. 38.
[22] M. Goldberg, Tohoku Math. J. 43 (1937) 104.
[23] J. Gray, Math. Intelligencer 4 (1982) 59.
[24] B. Grünbaum and T.S. Motzkin, Can. J. Math. 15 (1963) 744.
[25] R.C. Haddon, Acc. Chem. Res. 25 (1992) 127.
[26] J.M. Hawkins, A. Meyer, T.A. Lewis, S.D. Loren and F.J. Hollander, Science 252 (1991) 312.
[27] D. Hilbert and S. Cohn-Vossen, *Geometry and the Imagination* (Chelsea Publishing, New York, 1952) pp. 183–204.
[28] S.T. Hyde, Z. Kristallograph. 179 (1987) 53.
[29] S.T. Hyde, Acta Chem. Scand. 45 (1991) 860.
[30] S.T. Hyde and S. Andersson, Z. Kristallograph. 170 (1985) 225.
[31] S.T. Hyde and S. Andersson, Z. Kristallograph. 174 (1986) 225.
[32] D.E.H. Jones, New Scientist 35(519) (1966) 245.
[33] R.B. King, *Beyond the Quartic Equation* (Birkhäuser, Boston, 1996).
[34] R.B. King, J. Chem. Educ. 73 (1996) 993.
[35] R.B. King, J. Phys. Chem. 100 (1996) 15 096.
[36] R.B. King, Mol. Phys. 92 (1997) 293.
[37] R.B. King and E.R. Canfield, Comput. Math. Appl. 24 (1992) 13.
[38] R.B. King and D.H. Rouvray, Theoret. Chim. Acta 69 (1986) 1.
[39] F. Klein, Math. Ann. 14 (1879) 428.
[40] F. Klein, *Vorlesungen über das Ikosaeder* (Teubner, Leipzig, 1884) part I, chapter 2.
[41] F. Klein, *Gesammelte Mathematischen Abhandlungen*, Vol. 3 (Springer, Berlin, 1923) pp. 90–136.
[42] D.J. Klein and X. Liu, J. Math. Chem. 11 (1992) 199.
[43] D.J. Klein and X. Liu, Int. J. Quantum Chem. Symp. 28 (1994) 501.
[44] B. Kostant, Proc. Natl. Acad. Sci. USA 91 (1994) 11 714.
[45] B. Kostant, Notices Amer. Math. Soc. 42 (1995) 959.
[46] W. Krätschmer, L.D. Lamb, K. Fostiropoulos and D.R. Huffman, Nature 347 (1990) 35.
[47] H.W. Kroto, Angew. Chem. Int. Ed. 31 (1992) 111.
[48] H.W. Kroto, A.W. Allaf and S.P. Balm, Chem. Rev. 91 (1991) 1212.
[49] H.W. Kroto, J.R. Heath, S.C. O'Brien, R.F. Curl and R.E. Smalley, Nature 318 (1985) 62.
[50] T. Lenosky, X. Gonze, M. Teter and V. Elser, Nature 355 (1992) 333.
[51] X. Liu, T.G. Schmalz and D.J. Klein, Chem. Phys. Lett. 188 (1992) 550.

[52] A.L. Mackay and H. Terrones, Nature 352 (1991) 762.
[53] A.L. Mackay and H. Terrones, Phil. Trans. Roy. Soc. Lond. Ser. A 343 (1993) 113.
[54] D.E. Manolopoulos, D.R. Woodall and P.W. Fowler, J. Chem. Soc. Faraday 88 (1992) 2427.
[55] C.L. Mantell, *Carbon and Graphite Handbook* (Interscience, New York, 1968).
[56] E.R. Neovius, *Bestimmung Zweier Spezieller Periodische Minimalflächen* (J.C. Frenkel & Sohn, Helsinki, 1883).
[57] M. O'Keeffe, G.B. Adams and O.F. Sankey, Phys. Rev. Lett. 68 (1992) 2325.
[58] E. Osawa, Kagaku (Kyoto) 25 (1970) 854; Chem. Abstr. 74 (1971) 75 698v.
[59] W.N. Reynolds, *Physical Properties of Graphite* (Elsevier, Amsterdam, 1968).
[60] T.G. Schmalz, W.A. Seitz, D.J. Klein and G.E. Hite, J. Am. Chem. Soc. 110 (1988) 1113.
[61] H.A. Schwarz, *Gesammelte Mathematische Abhandlungen* (Springer, Berlin, 1890).
[62] P.W. Stephens, L. Mihaly, P.L. Lee, R.L. Whetten, S.-M. Huang, R.F. Kaner, F. Diederich and K. Holczer, Nature 351 (1991) 632.
[63] A.J. Stone, Mol. Phys. 41 (1980) 1339.
[64] A.J. Stone, Inorg. Chem. 20 (1981) 563.
[65] A.J. Stone, Polyhedron 3 (1984) 1299.
[66] A.J. Stone and M.J. Alderton, Inorg. Chem. 21 (1982) 2297.
[67] A.J. Stone and D.J. Wales, Chem. Phys. Lett. 128 (1986) 501.
[68] A.C. Tang, F.Q. Huang, Q.S. Li and R.Z. Liu, Chem. Phys. Lett. 227 (1994) 579.
[69] D. Vanderbilt and J. Tersoff, Phys. Rev. Lett. 68 (1992) 511.
[70] Z. Yoshida and E. Osawa, *Aromaticity* (Kagakudojin, Kyoto, 1971) pp. 174–178.